Journal of Sound and Vibration (1998) **209**(5), 882–888

ON THE DYNAMIC STABILITY OF RECTANGULAR PLATES SUBJECTED TO INTERMEDIATE FOLLOWER FORCES

J. H. Kim and J. H. Park

Department of Aerospace Engineering, Seoul National University, Kwan-Ak Ku, Seoul, Korea 151-742

(*Received* 29 *January* 1996, *and in final form* 25 *August* 1997)

1. INTRODUCTION

When large space structures need to change orbits or move to indicated positions, it may be thrusted. In such cases, plate-like structures may undergo dynamic instability due to bending by follower forces. For plate type structures, many researchers have studied the dynamic stability [1–6]. Studies on all free-edges rectangular plate structures under end follower forces have been performed by Higuchi *et al*. [7–9], but intermediate follower force cases have not been investigated.

Now, we investigate the dynamic stability of a rectangular plate which is subjected to intermediate follower forces. If a follower force is acting at the intermediate section of a plate, two regions of the plate must be considered. One region undergoes compressive load distribution, and the other region undergoes tensile load distribution because of plate inertia force distribution. In this study, with the changing of the acting line position of the intermediate force, the dynamic stability of the rectangular plate will be reported. In addition, the change of the dynamic stability property will be investigated with the change of the aspect ratio of the plate.

2. THEORY

Figure 1 shows the free–free plate model subjected to follower forces at intermediate section, and the follower force has constant value q per unit width.

In classical plate theory, kinetic energy is as follows:

$$T = \frac{1}{2}\int_0^b \int_o^a \bar{m}\left(\frac{\partial w}{\partial t}\right)^2 \mathrm{d}x\ \mathrm{d}y \tag{1}$$

where, $\bar{m}$ is mass of the plate per unit area, t is time and w is the plate deformation.

Strain energy is

$$U = \frac{1}{2}\int_0^b \int_0^a \left(D\left\{(\nabla^2 w)^2 + 2(1-\nu)\left[\left(\frac{\partial^2 w}{\partial x\,\partial y}\right)^2 - \frac{\partial^2 w}{\partial x^2}\frac{\partial^2 w}{\partial y^2}\right]\right\}\right) \mathrm{d}x\ \mathrm{d}y \tag{2}$$

When follower force q acts on the intermediate section of the plate, potential energy is as follows:

$$V = -\int_0^a \int_0^b q\ \mathrm{sign}\left(\frac{x}{a}\right)\left(\frac{\partial w}{\partial x}\right)^2 \mathrm{d}x\ \mathrm{d}y \tag{3}$$

0022–460X/98/050882 + 07 $25.00/0/sv971274

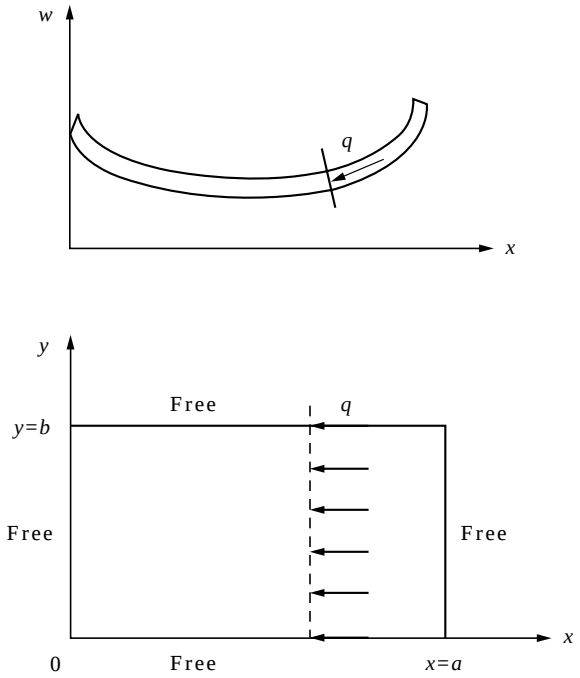

Figure 1. Plate model under intermediate follower forces.

where

$$\text{sign}\,(x) = \begin{cases} x & (0 \leqslant x < \alpha) \\ -1 + x & (\alpha < x \leq 1) \end{cases}$$

and α is the non-dimensional parameter ($0 \leqslant \alpha \leqslant 1$) which indicates the acting location of the follower force.

In the intermediate follower force case, load distribution must be considered in terms of two regions, as shown in Figure 2, i.e., compressive and tensile regions.

Non-conservative virtual work done by non-conservative component of q is as follows:

$$\delta W_{NC} = -\int_0^b \int_0^a q(\partial w/\partial x)\overline{\delta}(x - \alpha a)\delta w \, \mathrm{d}x \, \mathrm{d}y \tag{4}$$

where $\overline{\delta}(x - \alpha a)$ is Dirac's delta function.

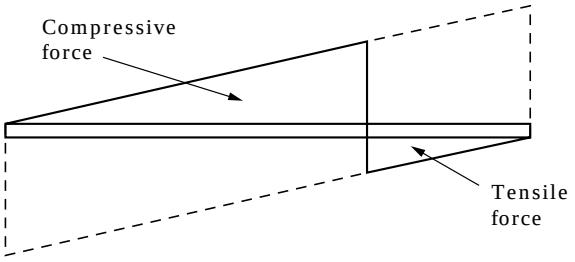

Figure 2. Axial load distribution for the intermediate follower force.

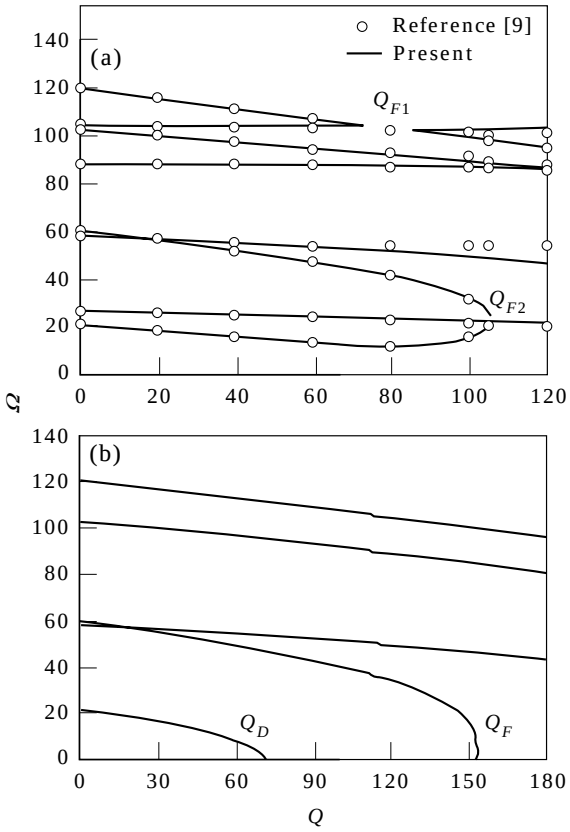

Figure 3. Eigenvalue curves: (a) end follower force ($\alpha = 1{\cdot}0$); (b) intermediate follower force ($\alpha = 0{\cdot}75$).

For a classical plate theory, Hamilton's principle can be written as

$$\int_{t1}^{t2} (\delta T - \delta U - \delta V + \delta W_{NC})\, \mathrm{d}t = 0 \tag{5}$$

By introducing Hamilton's principle and assuming $w(x, y, t) = w(x, y)\, \mathrm{e}^{i\omega t}$, we obtain eigenvalue equations as follows;

$$\det[-\bar{\omega}^2 \bar{\mathbf{M}} + \bar{\mathbf{K}} + \bar{\mathbf{Q}}] = 0 \tag{6}$$

where $\bar{\mathbf{M}}$ is mass matrix, $\bar{\mathbf{K}}$ is strain energy stiffness matrix, and $\bar{\mathbf{Q}}$ is stiffness matrix due to q.

When we introduce non-dimensional parameters such as

$$\xi = x/a, \qquad \eta = y/b, \qquad \lambda = a/b, \qquad \Omega^2 = \bar{m}\bar{\omega}^2 a^4/D, \qquad Q = qa^2/D \tag{7}$$

Then, equation (6) can be written in the normalized form as,

$$\det(-\Omega^2 \mathbf{M} + \mathbf{K} + Q\mathbf{G}) = 0 \tag{8}$$

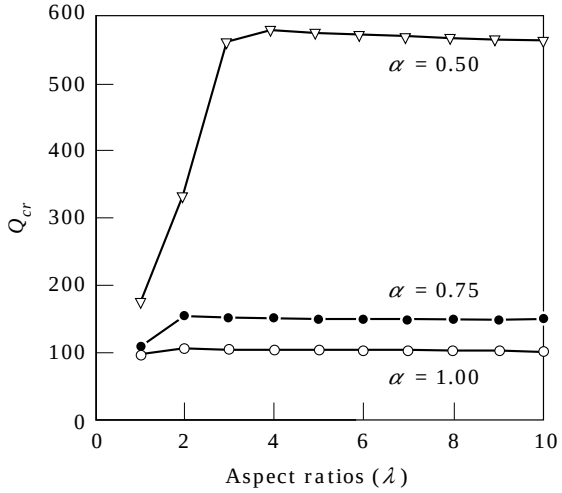

Figure 4. Critical load (Q_{cr}) versus aspect ratios (λ) ($1{\cdot}0 \leqslant \lambda \leqslant 10{\cdot}0$).

where

$$\mathbf{M} = \int_0^1 \int_0^1 w\delta w \, \mathrm{d}\xi \, \mathrm{d}\eta$$

$$\mathbf{K} = \int_0^1 \int_0^1 \left[\left(\frac{\partial^2 w}{\partial \xi^2} + \lambda^2 \frac{\partial^2 w}{\partial \eta^2} \right) \left(\frac{\partial^2 \delta w}{\partial \xi^2} + \lambda^2 \frac{\partial^2 \delta w}{\partial \eta^2} \right) + 2(1-v)\lambda^2 \left\{ \frac{\partial^2 w}{\partial \xi \, \partial \eta} \frac{\partial^2 \delta w}{\partial \xi \, \partial \eta} - \frac{1}{2} \left(\frac{\partial^2 w}{\partial \xi^2} \frac{\partial^2 \delta w}{\partial \eta^2} + \frac{\partial^2 w}{\partial \eta^2} \frac{\partial^2 \delta w}{\partial \xi^2} \right) \right\} \right] \mathrm{d}\xi \, \mathrm{d}\eta$$

$$\mathbf{G} = -\int_0^1 \int_0^1 \mathrm{sign}\,(\xi) \left(\frac{\partial w}{\partial \xi} \right) \frac{\partial \delta w}{\partial \xi} \, \mathrm{d}\xi \, \mathrm{d}\eta + \int_0^1 \frac{\partial w}{\partial \xi} \, \delta w|_{\xi = \alpha} \, \mathrm{d}\eta$$

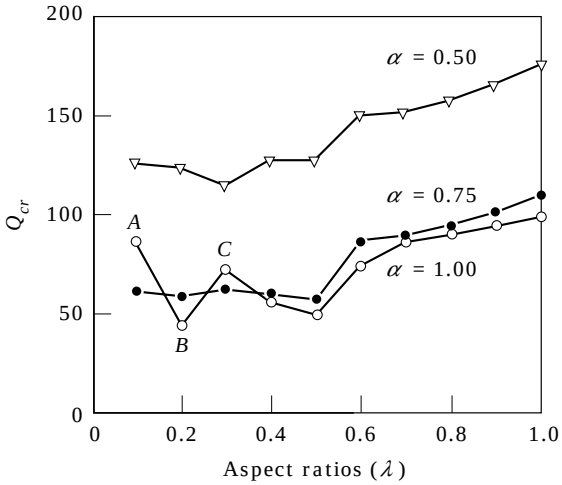

Figure 5. Critical load (Q_{cr}) versus aspect ratios (λ) ($0{\cdot}1 \leqslant \lambda \leqslant 1{\cdot}0$).

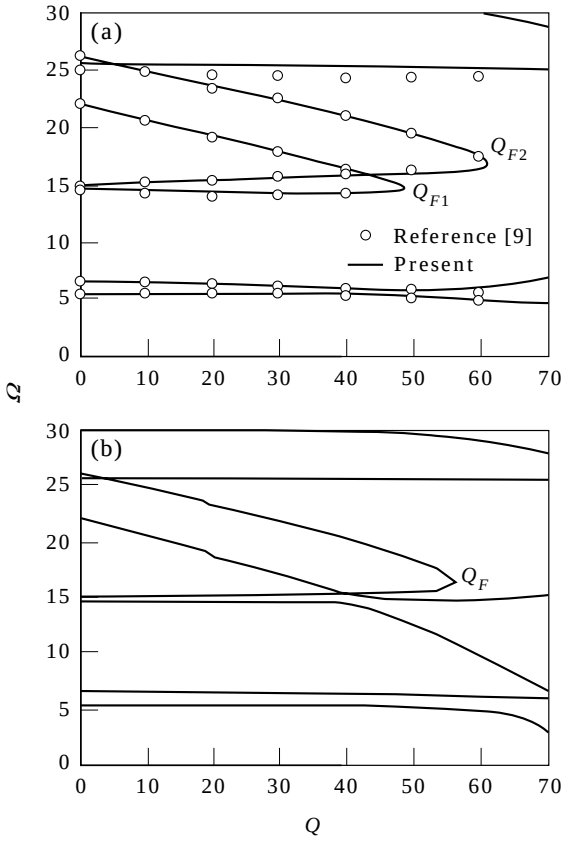

Figure 6. Eigenvalue curves ($\lambda = 0{\cdot}5$): (a) end follower force ($\alpha = 1{\cdot}0$); (b), intermediate follower force ($\alpha = 0{\cdot}75$).

From the above expression of **K**, we can realize that the element with C^1 continuity must be used. Thus, in the present study, the Hermite element is used in the finite element formulation.

3. RESULT

We observed that the critical load for the dynamic stability for 4×4 elements model was different only by 1% or so from that of 6×6 elements model. Hence, from now on, we will examine the dynamic stability based on the results by using the 4×4 elements model.

The dynamic stability of a thin plate is known to be very sensitive to aspect ratios. Now, we will investigate the transition of critical load value for dynamic stability with respect to the change of aspect ratios.

3.1. *Large aspect ratio case*

Figure 3 shows eigenvalue curves in the case of $\lambda = 2{\cdot}0$ and $\nu = 0{\cdot}3$, where λ is the aspect ratio. The lowest three eigenvalues are all zeros, corresponding to rigid body modes and they do not cause any destructive behavior to the structure. So, the rigid body modes are not illustrated. Figure 3(a) is the end edge follower force case ($\alpha = 1{\cdot}0$) and is in accordance with the result of reference [9]. As shown in this figure, there are critical load Q_{F1} indicating

weak dynamic instability and Q_{F2} indicating strong dynamic instability. Although instability exists after Q_{F1}, the value of the imaginary part of eigenvalue is very small and unstable behavior is maintained temporarily. Compared with the case Q_{F2}, Q_{F1} is not important and weak stability often vanishes when structural damping is considered. On the other hand, weak stability doesn't appear in Figure 3(b) which is the case of intermediate follower force case at 3/4 section of the plate. Compared with the end follower force case, Figure 3(b) shows that the value of the critical load for dynamic instability becomes larger though divergence by one of the eigenvalues becoming zero first.

Figure 4 shows the critical loads for varying aspect ratios from 1 to 10 in the case $v = 0{\cdot}3$. Generally, the more the tensile region increases, the larger the value of critical force for dynamic stability grows.

3.2. *Small aspect ratio case*

Figure 5 shows critical loads with varying aspect ratios ranging from 0·1 to 1·0. Here, the end follower force case ($\alpha = 1{\cdot}0$) intersects with the intermediate follower force case ($\alpha = 0{\cdot}75$) which is different from the case in section 3.1. This means that it is not always true that large tensile regions cause the increase of dynamic stability. In the small aspect ratio case, critical forces do not follow a smooth curve, and change radically with small changes of aspect ratio. This is due to the fact that the two modes which cause dynamic instability by converging as complex conjugate are not constant and can be changed by small aspect ratio change, therefore, the critical load does not have a constant tendency. The two modes which determine dynamic instability can be regarded as the characteristic of dynamic instability for this aspect ratio region. If the interval of aspect ratio in Figure 5 is denser, more intersect points may be shown. From Figure 5 we can say that in this aspect ratio region, the characteristic of this system is affected by the change of location of follower force as well as aspect ratio of the plate. Hence, sometimes the value of the critical load in more tensile region cases can be much smaller than that of less tensile region cases. But, in this case, the stability for the $\alpha = 0{\cdot}5$ case increases distinctly.

Figure 6 shows eigencurves in the $\lambda = 0{\cdot}5$ case. In Figure 6(a), as the end follower force case, third and fifth eigenvalues meet each other and bring about the first dynamic instability. However, in Figure 6(b), for the intermediate follower force case at $\alpha = 0{\cdot}75$, the third and fifth eigenvalues which cause dynamic instability in Figure 6(a) do not meet each other. In addition, the two eigenvalues which make second dynamic instability in Figure 6(a) cause first dynamic instability with a smaller value of critical force in Figure 6(b). Though the value of critical load is smaller in the end follower force case, the two modes which cause first dynamic instability are different in two cases. Hence, it is considered that each case must be examined with extra attention.

4. CONCLUSION

The analysis of a completely free plate subjected to intermediate follower force can be summarized as follows.

In the large aspect ratio range, the more the tensile region grows, the more the dynamic stability increases due to the fact that the cause of dynamic instability is bending due to compressive loading. In addition, as aspect ratio grows, the value of critical force converges at a constant value which is in accordance with the beam model. So, in the case of sufficiently large values such as 10, the plate can be considered as a beam.

In a small aspect ratio range, it cannot be said that the dynamic stability increases in proportion to tensile region of the plate. In this case, the characteristic of dynamic stability is very sensitive to the change of aspect ratio and the location of follower force. Hence,

as the value of critical load for dynamic instability varies with the location of follower force, it is considered that each case must be examined with extra attention.

REFERENCES

1. Z. Celep 1979 *Journal of Sound and Vibration* **65**, 549–556. Axially symmetric stability of a completely free circular plate subjected to a non-conservative edge load.
2. Z. Celep 1982 *Journal of Sound and Vibration* **80**, 421–431. Vibration and stability of a free circular plate subjected to a non-conservative loading.
3. H. H. E. Leipholz and F. Pfendt 1982 *Computer Methods in Applied Mechanics & Engineering* **30**, 19–52. On the stability of rectangular, completely supported plates with uncoupling boundary conditions subjected to uniformly distributed follower forces.
4. H. H. E. Leipholz and F. Pfendt 1983 *Computer Methods in Applied Mechanics & Engineering* **37**, 341–365. Application of extended equations of Galerkin to stability problems of rectangular plates with free edges and subjected to uniformly distributed follower forces.
5. L. W. Chen and J. Y. Yang 1990 *Computer & Structure* **36**, 845–851. Dynamic stability of laminated composite plates by the finite element method.
6. C. L. Liao and Z. Y. Lee 1993 *International Journal for Numerical Methods in Engineering* **36**, 1825–1847. Elastic stability of skew laminated composite plates subjected to biaxial follower forces.
7. K. Higuchi and E. H. Dowell 1990 *American Institute of Aeronautics and Astronautics Journal* **28**, 1300–1305. Dynamic stability of a rectangular plate with four free edges subjected to a follower force.
8. K. Higuchi and E. H. Dowell 1992 *American Institute of Aeronautics and Astronautics Journal* **30**, 820–825. Effect of structural damping on flutter of plates with a follower force.
9. K. Higuchi and E. H. Dowell 1989 *Journal of Sound and Vibration* **129**, 255–269. Effects of the poisson ratio and negative thrust on the dynamic stability of a free plate subjected to a follower force.